

# Measurement and FEMM Modelling of Experimentally Generated Strong Magnetic Fields

Nasser Bashir Ekreem<sup>1</sup>, Mohamed A. S. Hassan<sup>2</sup>, Nasar Aldian Ambark Shashoa<sup>3</sup>,  
Abdurrezag S. Elmezughi<sup>4</sup>.

<sup>1,2,3,4</sup>(Electrical Engineering Department, Azzaytuna University / Faculty of Engineering, Tarhuna, Libya)

## Abstract:

This work presents correlations between experimentally generated magnetic field strengths and computationally modeled field strengths. The experimental set-up comprised a C-shape structure designed to generate strong magnetic field strengths. The sections of the C-structure were individual solenoids made from copper-wound low carbon steel. These sections were connected such that the overall structure formed a continuous conduit for the magnetic flux and concentrated the magnetic field into an air gap. This experimental set-up could be used for magnetic annealing, or alternatively to measure the magnetostrictive strain properties of suitable materials, placed in the air gap. Magnetic field strengths of approximately 1.0 Tesla (T) were measured using a magnetic field strength meter. Finite Element Method Magnetics (FEMM) computational modeling software was used to model the design and predict field strengths. Modeled field strengths fell short of practical measurements. The efficiency of the apparatus in producing high fields is reduced due to effects related to drilling and machining of the steel core. Other reasons for discrepancies include the configuration of the C-shape, the properties of the core material, and skin effects. By building these considerations into the FEMM model, a more accurate representation of the workings of the C-shape set-up was achieved.

**Keywords** —Magnetic field strength, Magnetic circuit design, Finite Element Method Magnetics (FEMM).

## I. INTRODUCTION

This High magnetic fields can be generated in several ways such as electromagnets (iron-core solenoids and air-core solenoids), pulsed magnets, and superconducting magnets. In selecting a magnet for use in a particular application, the most important considerations are the magnitude of the magnetic field required, and the power available. Air-core solenoids require higher power input in order to produce high magnetic fields at the centre of the solenoids, compared with iron-core solenoids. The first iron-core electromagnet was built and demonstrated by Sturgeon by wrapping a conductor around a horseshoe-shaped bar of iron and passing a current through the winding. One of the original air-core magnet designs was developed by Montgomery [1]. This design was capable of generating 250 kilogauss, and required a power input of 12 megawatts. The system was made up of

three coaxial solenoids. A water-cooling system was used at a rate of 3000 gal/min in order to eliminate the heat generated in each coil. Modern day, iron-core electromagnets can produce static magnetic field strengths of up to 20 kOe. Normally the magnetic circuit comprises a yoke and two high permeability low carbons steel. Coils of wire having thousands of windings are assembled around the iron cores. The useful magnetic field is produced in the air-gap. This magnetic field is greatly affected by the magnitude of the current supplied to the coils, the permeability of the iron core, and the physical dimensions of the magnetic circuit (in particular the air- gap distance and length of the core). The coils are water or air-cooled in order to avoid damage to the insulating material around the copper wire. Important specifications of electromagnets include; maximum magnetic field produced in the air gap, power consumption, maximum current, and cooling mechanism and flow

rates (water or air). Magnetic fields in the range 100 to 400 kOe can be accomplished by means of pulsed magnets. These systems are based on the discharge of the energy stored in a battery of condensers. Using this technique, Jana et al. applied a DC voltage of 2.5 kV across the capacitor bank to produce a magnetic field of nearly 8 T [2]. Superconducting magnets consist of solenoids made of superconducting coils. The coil windings are made of wires of Type II superconductor (e.g. niobium titanium). The solenoid must be cooled in liquid-helium. These magnets are able to support a very high current density with a very small resistance and little or no electrical power input. Ozaki et al. designed a superconducting magnet that is composed of Nb<sub>3</sub>Sn and NbTi conductors [3]. The central magnetic field of this magnet is 17 T. Cryogen-free superconducting magnets (CFM) are based on Gifford-McMahon refrigerators. These electromagnets require no liquid-helium. This cryogen-free technology represents an important breakthrough since liquid-helium is expensive and difficult to obtain. Nowadays, a growing number of cryogen-free magnets are under development around the world. Based on this technology, cryogen-free magnets in the range 18 to 20 T can be produced. Another way of generating high magnetic fields is to use a vibrating sample magnetometer (VSM). VSM's mainly consist of an electromagnet, a vibrator mechanism to vibrate a sample in the magnetic field, and detection coils which generate the signal voltage due to the changing flux emanating from the vibrating sample. The magnetic field is generated by an electromagnet driven by a DC bipolar power supply. If much stronger magnetic fields are required, the electromagnet can be replaced by a superconducting solenoid which significantly increases the operational cost and time of measurement. Recently, Lo et al. used a VSM to generate a static magnetic field of 4000 Oe [4]. This technique was employed to magnetically anneal cobalt ferrite ceramic. The purpose of the apparatus presented here is to generate a strong and static magnetic field which can be used to carry out magnetostrictive strain testing of magnetostrictive materials, such as nickel, Terfenol-D and cobalt ferrite [5]. In the case of non-static magnetic fields, various electrostatic effects can occur, not only

complicating the analysis of the system, but also releasing energy losses due to eddy currents.

## II. EXPERIMENTAL SET-UP

The experimental set-up comprised a C-shape structure designed to generate strong magnetic field strengths. The initial C-shape circuit design consisted of three separate coils wound around a low-carbon steel core (30 mm in diameter) as depicted in Fig 1. The three coils were connected using four corners made of pure iron to form a continuous conduit for the magnetic flux. Each coil consisted of 8,000 turns arranged in ten layers. These layers were wired in a semi-series/semi-parallel wiring arrangement. Winding of the wire was carried out using a computer numerical control (CNC) lathe. To minimize the heat generated in each coil, it was necessary to insert layers of copper tubes with outside diameters of 3 mm between every two layers of windings as shown in Fig 2.

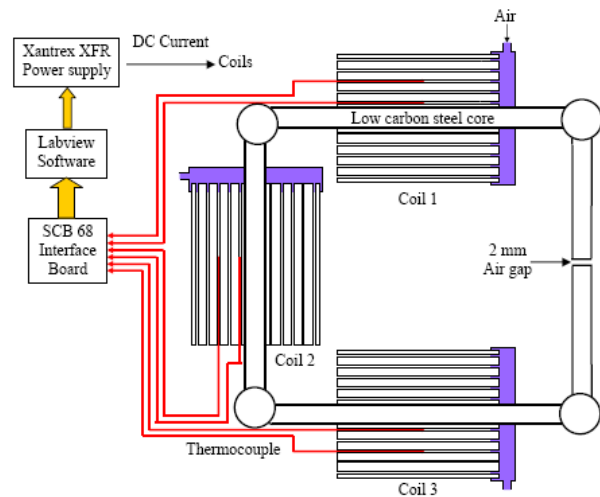


Fig. 1 Initial experimental set-up of the C-shape electromagnetic rig.

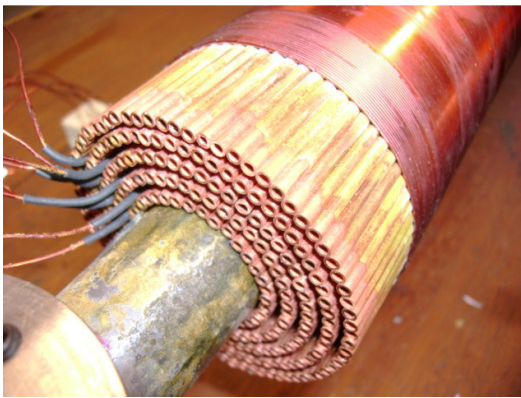


Fig. 2 Distribution of copper tubes.

Compressed air was forced through the tubes at a pressure of 4 bar. In each coil, two temperature probes (thermocouple type K) were positioned; one between the first and second layer of windings, and the other probe between the fifth and sixth layer. A maximum temperature of approximately 40°C was reached with a steady current of 15 amps in each coil. The cooling system was therefore considered successful for currents of this magnitude. The temperature probes were interfaced with NI PCI\_6024E data acquisition card (DAQ) and Lab-View software. This DAQ card was used to export the temperature data, and also to control the current which was fed to the coils. A hand-held Hall Effect gaussmeter (Model 5180, Sypris Solutions Ltd., USA) was used to measure magnetic flux density. The active measuring part of the probe is close to the centre of the cross section. A Teflon (PTFE) plastic disc was made, measuring 2 mm in thickness by 30 mm in diameter. This custom-made plastic disc was placed and held in the 2 mm air gap. It has a notch which could accommodate the tip of the DC gaussmeter transverse probe which was used to measure the magnetic flux density. This ensured the same probe position for successive measurements. It also ensured that the active probe tip was always centered in the air gap. Xantrex™ XFR 150v, 18 Amps DC power supply (Xantrex™ Inc. Technology, Canada) was used as a current source. It is provided with RS-232 interface card, which gives remote digital control of the system. A maximum current of 15 amps was passed through each coil. For each measured value of magnetic flux

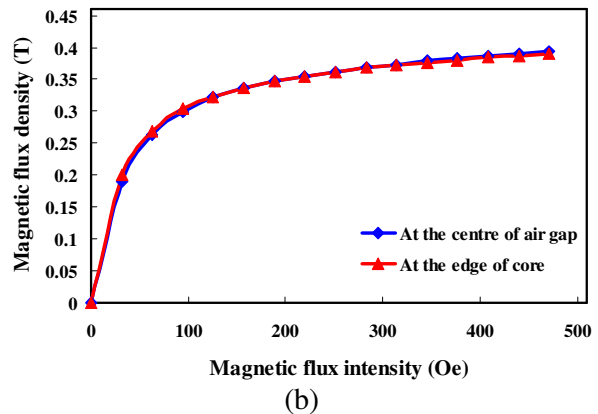
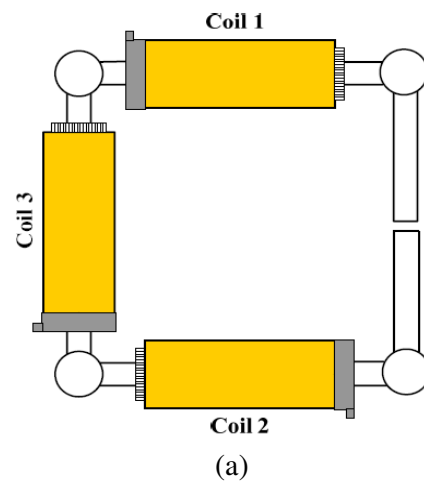
density, the corresponding magnetic field strength was calculated using the following formula:

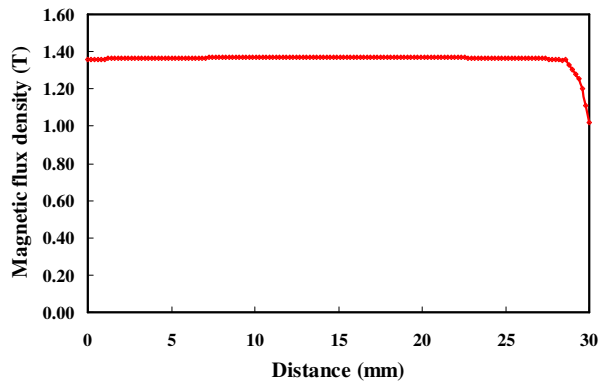
$$N \times I = \oint H dl \quad (1)$$

### III. RESULTS

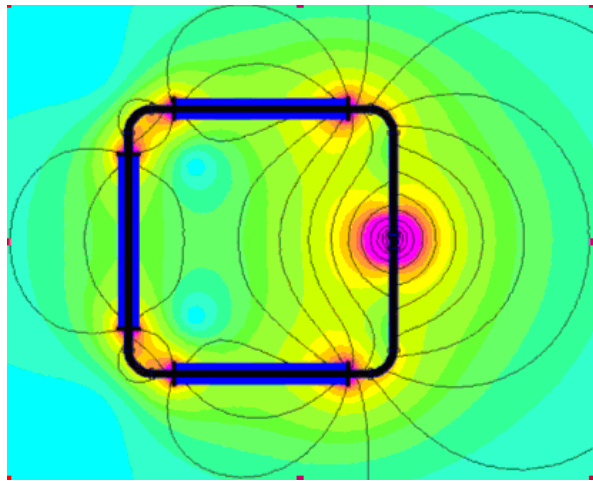
#### 1. First Configuration

The electromagnetic structure was assembled into two different configurations. Fig. 3(a) shows the first C-shape configuration. Fig. 3(b) shows the measured magnetic flux density across the air-gap. As shown, it reached ~ 0.4 T in the centre of the air-gap. The flux density predicted at the centre of the air-gap using FEMM for this configuration is shown in Fig. 2(c). Clearly, this is more than three times the measured value.





(c)



(d)

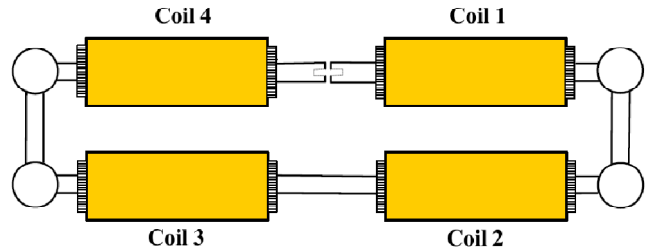
Fig. 3 Magnetic field strengths generated by the first configuration of the C-shape magnetic circuit.

It was assumed that a constant magnetic flux flows through the whole of the C-shape including its air-gap. However, Fig. 3(d) reveals that this is not strictly true. In fact, there is leakage of flux at various points in the circuit. There is some leakage at the corners of the iron core, but the largest leakage occurs at the air-gap, where magnetic flux lines can be seen to by-pass the air-gap. The extent of the flux leakage is difficult to estimate because the depiction tends to exaggerate the amount of leakage, making it difficult to visualise the amount of concentrated flux passing along the iron core.

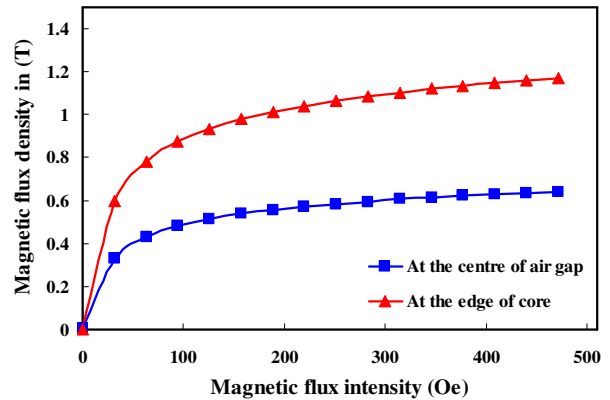
## 2. Second Configuration

### A. Screw Holes on The Surfaces Either Side of The Air-Gap

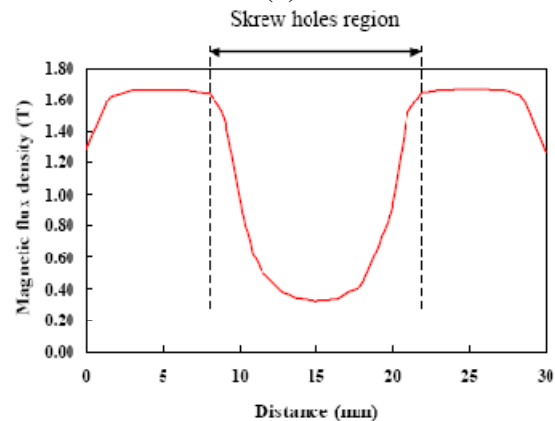
Fig. 4(a) reveals the second C-shape configuration. Measurements showed that the measured magnetic flux density was sensitive to the position of the magnetic field strength meter probe tip. The measured magnetic flux density reached ~ 0.6 T in the centre of the air-gap and 1.2 T at the edge of the core (Fig. 4(b)). The difference in values is due to the presence of screw holes in the surfaces either side of the air-gap. Both values are more than the value recorded for the first configuration.. However, This value still fell short of expected.



(a)



(b)



(c)

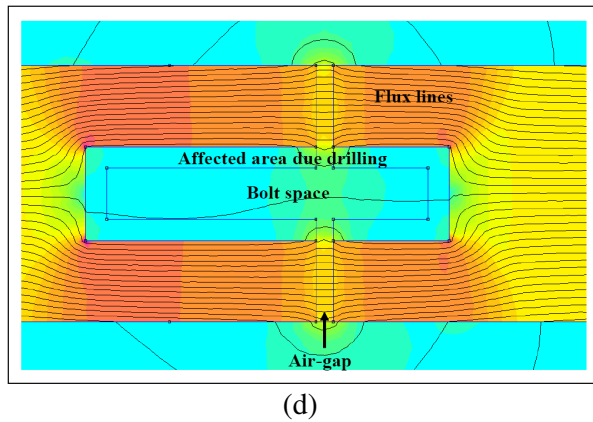


Fig 4 Second configuration of the electromagnetic rig with screw holes in the flat surfaces either side of the air-gap

The reason for the low experimentally-measured value could be due to loss of flux at the core joints; due to screw holes where the corners are bolted together, or due to prior machining of the core itself [6-7]. When the system was modelled in FEMM, the magnetic flux lines seemed to by-pass the screw holes (Fig. 4(d)), causing the flux density to be decreased to ~ 0.4 T at the centre compared to ~ 1.6 T at the edges as depicted in Fig. 4(c). The reason for this difference in values is due the effect of the presence of the screw hole.

### B. Flat Surfaces on Either Side of The Air-Gap With Buried Screw Holes

In an attempt to assess the impact of buried screw holes between the surfaces either side of the air-gap, flat spacers were added to cover both screw holes as shown in Fig. 5(a). As a result, the measured magnetic flux density increased to 0.9 T in both the centre of the air-gap and the edge of the core (Fig. 5(b)).

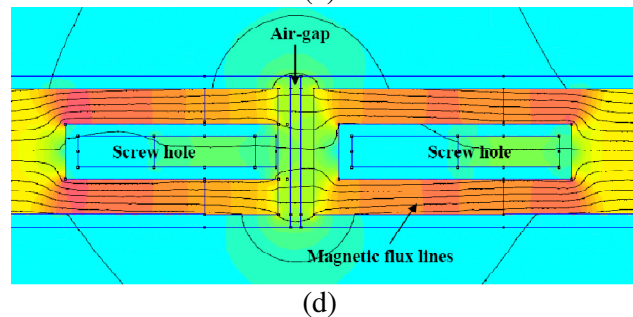
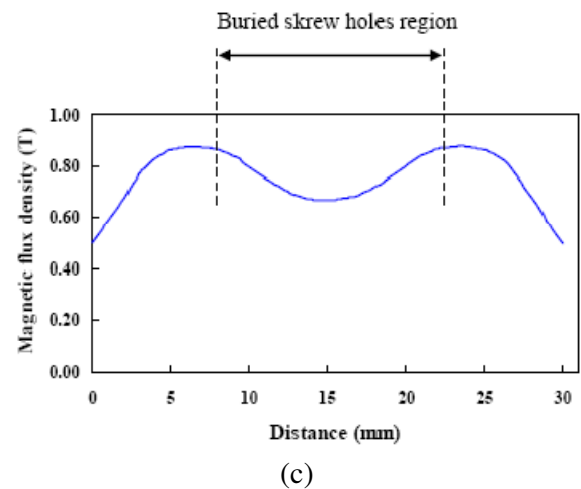
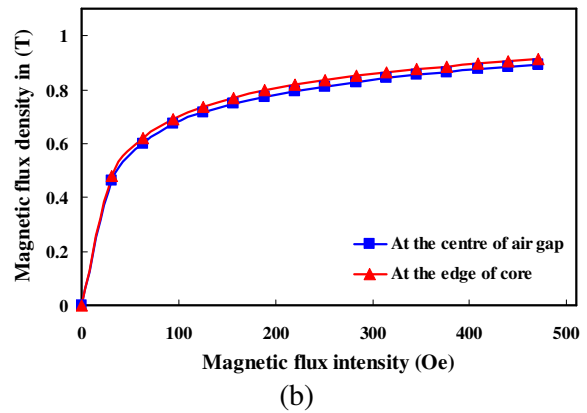
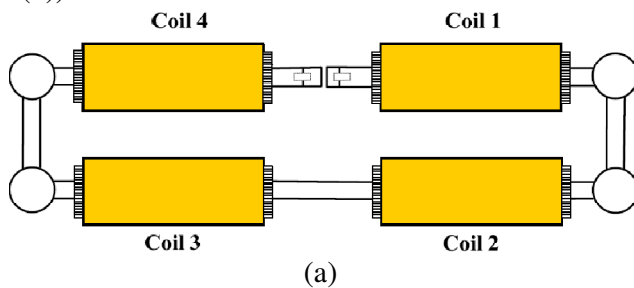


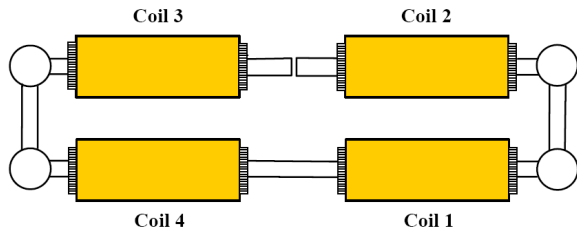
Fig. 5 Second configuration of the electromagnetic rig with flat surfaces on either side of the air-gap and buried screw holes

This value is more than double the value achieved in the first configuration. This is believed due to the proximity of the coils to the air-gap for the second configuration. When this was modelled in FEMM, the magnetic flux lines seemed to by-pass the screw holes (Fig. 5(d)), causing the flux density around the bolted area to decrease as depicted in Fig. 5(c). In an attempt to assess the impact of prior machining on the iron core, a “skin effect” was

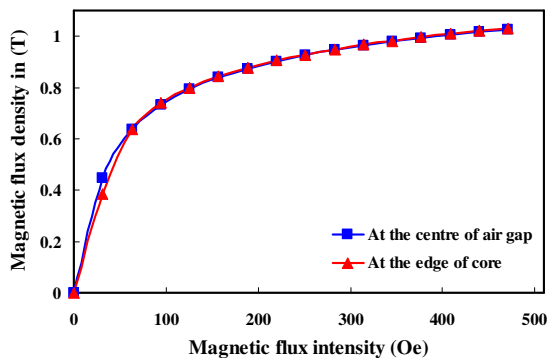
introduced into the outer 2.5 mm in FEMM around the corners and bolted areas. This resulted in only a minor reduction in flux density at the centre of the air-gap to 0.7 T as shown in Fig. 5(c).

### C. Flat Surfaces on Either Side of The Air-Gap With no Buried Screw Holes

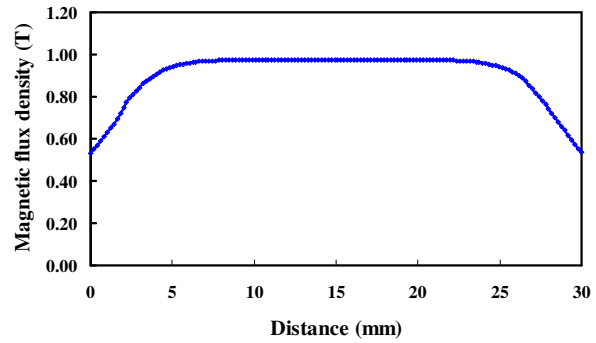
To eliminate the effect of the buried screw holes, the air-gap was located between the second coil and third coil where the surfaces on either side of the air-gap are flat with no buried screw holes as shown in Fig. 6(a). The measured magnetic flux density at the centre and edge was increased to 1.0 T (Fig. 6(b)). This value is in a good agreement with the predicted value resulted in FEMM which was 1.0T as illustrated in Fig. 6(c).



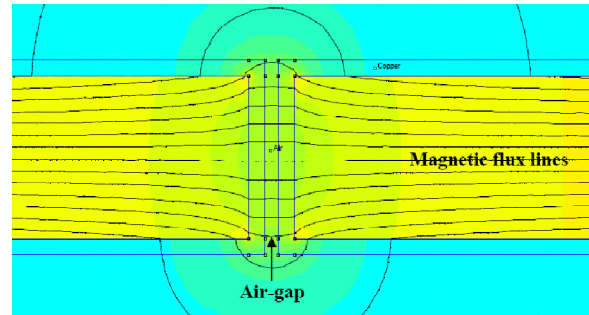
(a)



(b)



(c)



(d)

Fig. 6 Second configuration of the electromagnetic rig with flat surfaces on either side of the air-gap and no buried screw holes

This increase in the magnetic flux density is due the absence of any screw holes in the core near the air-gap, and the magnetic flux lines can penetrate the air-gap with less reluctance as shown in Fig. 6(d).

### IV. CONCLUSIONS

Finite Element Method Magnetics (FEMM) computational modelling software was used to predict magnetic field strengths generated by an electromagnetic rig. Two different configurations were investigated. In this way, the arrangement of the coils was shown to greatly affect the resultant magnetic field strength. By arranging the coils closer to the air-gap, greater field strengths were recorded. According to FEMM analysis, the efficiency of the electromagnetic rig in producing high magnetic fields can be decreased due to effects related to drilling and machining of the steel cores, especially when drilling is carried near or at the air-gap. Other reasons for discrepancies include flux leakages and skin effects in the core material. By building these considerations into the FEMM model,

modelled values approached the experimentally measured ones.

## **REFERENCES**

- [1] Bitter F. New developments in high magnetic field research.  
<http://www.philsoc.org/1961Spring/1510transcript.html>. 2007.
- [2] Jana S, Mukherjee RK, Generation and measurement of pulsed high magnetic field. J. Magn. Mater. 2000; 214: 234-42.
- [3] Ozaki O, Koyanagi K, Kiyoshi T, Matsumoto S, Fujihira J, Wada H, Development of superconducting magnets for uniform and high magnetic force field generation, IEEE Trans. Appl. Superconductivity 2002; 12: 940-3.
- [4] Lo CH, Ring A, Snyder J, Jiles D, Improvement of magnetomechanical properties of cobalt ferrite by magnetic annealing, IEEE Trans. Magn, MAG 2005; 41: 3676-8.
- [5] Ekrem N., et al.: An overview of magnetostriction, its use and methods to measure these properties", J. Mater. Process. Tech., 2007, pp. 96-101
- [6] Bas J. A. , Molins C. Jr, Effect of machining procedures on the magnetic properties of several sintered soft magnetic materials. PM'86 proceedings.
- [7] Maxime R. Dubois, Patrick Lemieux, Charles Cyr, and Daniel Massiocotte, Effect of machining on the properties of resin-based soft magnetic composites. ICEM Greece 2006.